ORNL/TM-2014/380

# Advanced ODS FeCrAl Alloys for Accident-Tolerant Fuel Cladding


Sebastien Dryepondt
Kinga A. Unocic
David T. Hoelzer
Bruce A. Pint

**August 29, 2014**



OAK RIDGE NATIONAL LABORATORY
MANAGED BY UT-BATTELLE FOR THE US DEPARTMENT OF ENERGY

**ORNL/TM-2014/380**

FCRD Advanced Fuels Campaign

# Advanced ODS FeCrAl alloys for accident-tolerant fuel cladding

Sebastien Dryepondt
Kinga A. Unocic
David T. Hoelzer
Bruce A. Pint

Date Published:

August 29, 2014

Prepared by
OAK RIDGE NATIONAL LABORATORY
Oak Ridge, Tennessee 37831-6283

managed by
UT-BATTELLE, LLC
for the
US DEPARTMENT OF ENERGY
under contract DE-AC05-00OR22725

**CONTENTS**

**Page**

## LIST OF FIGURES

**Figure** **Page**

## LIST OF TABLES

**Table** **Page**

## ABSTRACT

Oxide dispersion strengthened (ODS) FeCrAl alloys are being developed with optimum composition and properties for accident tolerant fuel cladding. Two ODS Fe-15Cr-5Al+$Y_2O_3$ alloys were fabricated by ball milling and extrusion of gas atomized metallic powder mixed with $Y_2O_3$ powder. To assess the impact of Mo on the alloys mechanical properties, one alloy contained ~1wt% Mo. The hardness and tensile properties of the two alloys were close and higher than the values reported for fine grain PM2000 alloy. This is likely due to the combination of a very fine grain structure and the presence of nano oxide precipitates. The nano oxide dispersion was, however, not sufficient to prevent grain boundary sliding at 800ºC and the creep properties of the alloys were similar or only slightly superior to fine grain PM2000 alloy. Both alloys formed a protective alumina scale at 1200ºC in air and steam and the mass gain curves were similar to curves generated with 12Cr-5Al+$Y_2O_3$ (+Hf or Zr) ODS alloys fabricated for a different project. To estimate the maximum temperature of use for the two alloys in steam, ramp tests at a rate of 5ºC/min were carried out in steam. Like other ODS alloys, the two alloys showed a significant increase of the mass gains at T~ 1380ºC compared with ~1480ºC for wrought alloys of similar composition. The beneficial effect of yttrium for wrought FeCrAl does not seem effective for most ODS FeCrAl alloys. Characterization of the hardness of annealed specimens revealed that the microstructure of the two alloys was not stable above 1000ºC. Concurrent radiation results suggested that Cr levels <15wt% are desirable and the creep and oxidation results from the 12Cr ODS alloys indicate that a lower Cr, high strength ODS alloy with a higher maximum use temperature could be achieved.

## 1. Introduction

The Fukushima accident has led to a renewed interest in advanced materials for accident-tolerant fuel cladding that could withstand very high temperature exposure in steam environments for several hours.[1,2] FeCrAl alloys are among the leading candidates because of their excellent oxidation behavior in steam at high temperature due to the formation of an adherent and protective alumina scale. [1-4] On going research at ORNL aims to develop new high temperature FeCrAl alloys with improved mechanical properties at the ~300°C operating temperature, and low (10-15%) alloy Cr content to avoid the formation of the brittle $\alpha$–Cr phase upon irradiation.[2,5-6] One key issue with FeCrAl cladding is that the transition from Zr-based alloys to an Fe-based alloy will result in a neutronic penalty.[2,7] One strategy to mitigate this penalty is for the cladding to have higher mechanical properties, which will allow for the design of a thinner tube cladding. Alloying additions and thermo-mechanical processing have successfully increased the strength of wrought FeCrAl alloys [8]. To further increase the mechanical properties at intermediate temperatures, and potentially increase the tube burst resistance at high temperature, nano oxide particles can be added to the FeCrAl alloy. Two oxide dispersion strengthened ODS Fe-15Cr-5Al+$Y_2O_3$ alloys were therefore fabricated, one of them containing ~1wt% Mo. The composition of the alloys was chosen based on previous work on wrought FeCrAl alloys showing that 15Cr and 5Al are sufficient to form a protective alumina scale at high temperature in steam. Previously, small additions of Mo were found to improve the mechanical properties of ODS Fe-10Al-5Cr alloys, [9] and FeCrTi alloys.[10-11]

The microstructure stability, mechanical properties and oxidation resistance of the two alloys have been evaluated and the results compared with similar results obtained from two commercial FeCrAl alloys, APMT and PM2000, and two ODS 12Cr-5Al+$Y_2O_3$ (+Hf or Zr) alloys developed at ORNL under funding from the Office of Fusion Energy.

## 2. Experimental procedure

### 2.1 Materials

Gas atomized Fe-15Cr-5Al-0.5Ti and Fe-15Cr-5Al-0.5Ti-1Mo powders, in weight percent, were purchased from ATI Metal Powders with a powder size ranging from 45 to 150μm. 1 kg of powder was ball milled in an Ar atmosphere for 40h with $Y_2O_3$ powder produced by Nanophase, Inc using a Zoz CM08 Simoloyer ball mill. The resulting powder was then degassed at 300ºC for 24h, sealed in a carbon steel extrusion can, and finally heated at 950ºC for 1h before extrusion. The composition of the alloys, designated 155YT and 155YMT, analyzed by inductively coupled plasma (ICP) spectroscopy, combustion, and inert gas fusion (IGF) analysis, are given in Table 1. The composition of the commercial alloys PM2000 and APMT and the ODS 12Cr-5Al alloys developed under a separate project are also included in Table 1.

Table 1: Alloys composition measured by ICP spectroscopy, combustion and IGF analysis

| Wt % | Fe | Cr | Al | Ti | Y | Si | C (ppm) | N (ppm) | O (ppm) | S (ppm) | Other |
|---|---|---|---|---|---|---|---|---|---|---|---|
| 155YT | bal. | 14.57 | 4.7 | 0.44 | 0.16 | 0.02 | 340 | 240 | 951 | 10 | |
| 155YMT | bal. | 14.55 | 4.75 | 0.44 | 0.16 | 0.02 | 370 | 128 | 828 | <10 | 0.88 Mo |
| PM2000 | 74.12 | 19.13 | 5.46 | 0.48 | 0.39 | 0.02 | 14 | 86 | 2480 | 8 | |
| APMT | 69.16 | 21.06 | 4.99 | 0.02 | 0.25 | 0.59 | 300 | 402 | 526 | <10 | 2.82 Mo, 0.23Hf 0.1Zr |
| 125YZ | 82.8 | 11.51 | 4.86 | <0.01 | 0.18 | 0.01 | 250 | 161 | 1920 | 10 | 0.3Zr, 0.01Hf |
| 125YH | 82.3 | 11.68 | 4.82 | <0.01 | 0.17 | 0.01 | 220 | 110 | 2280 | 10 | 0.68Hf, 0.01Zr |

### 2.2 Annealing experiments

Coupons ~10x10x1.5mm machined from the extruded materials and commercial alloys were exposed for 1000h at 800ºC, 1h, 100h and 1000h at 1000ºC, and 1h and 100h at 1200ºC to assess the alloy microstructure stability. For the 1000h exposure, larger rectangular blocks ~25x10x10mm were also annealed to allow for the machining of tensile specimens. All of the samples were placed in sealed quartz ampoules backfilled with an Ar-4%$H_2$ mixture to avoid oxidation during annealing.

### 2.3 Creep and tensile testing

Sub-sized sheet tensile specimens (SS-3) 7.62 mm long and with a 0.762 or 1 mm thick gage section were machined along the extrusion direction. Tensile testing was conducting from 20 to 800ºC with an MTS hydraulic frame at a $10^{-3}s^{-1}$ deformation rate. The creep specimens were very similar in shape but with a gage section of 2x2mm. Creep testing was conducted at 800ºC on a dead load machine with the specimen deformation being measured using an extensometer equipped with two LVDTs. Type S thermocouples located at the bottom and top heads of the specimens were used to control the temperature within 3ºC.

### 2.4 Oxidation testing

Rectangular oxidation coupons, ~20x10x1-1.5mm in size, were polished to a 600 grit surface finish and then cleaned in acetone and methanol. Isothermal oxidation experiments were conducted at 1200ºC using a magnetic suspension Rubotherm DynTHERM thermogravimetric analyzer (TGA). The tests were conducted either in dry air or 100% steam. Ramp tests were also conducted in steam using the same TGA,

with the temperature being increased at a rate of 5ºC/min to 1500°C or until a mass gain greater than ~2mg/cm$^2$ was measured.

### 2.5 Microstructure characterization

As extruded and annealed coupons were mounted in epoxy and then polished using standard metallography procedures. The microstructure was then characterized using a JEOL model 6500 Field Emission Gun Scanning Electron Microscope (FEG-SEM). It was not feasible to perform TEM after all conditions. Therefore, hardness was used as an indication of the microstructure stability. The Vickers hardness was measured using a 100 or 500 g load. The average grain size was obtained by the line intercept method in terms of the 95-percent confidence interval around the mean.

## 3. Results

### 3.1 As extruded material

As can be seen in Figure 1a-d, the fine grain structure observed after extrusion of the two alloys was not perfectly homogeneous. In most areas, the average grain size was 0.55μm for alloy 155YT and 0.86μm for alloy 155YMT, but areas with larger grains were also present, up to ~50μm in size for alloy 155YT. A network of alumina stringers was also observed in both alloys. As expected, Figure 1c-d shows the presence of small precipitates <20nm in size, and TEM characterization is in progress to quantify the precipitates size, density and phase.

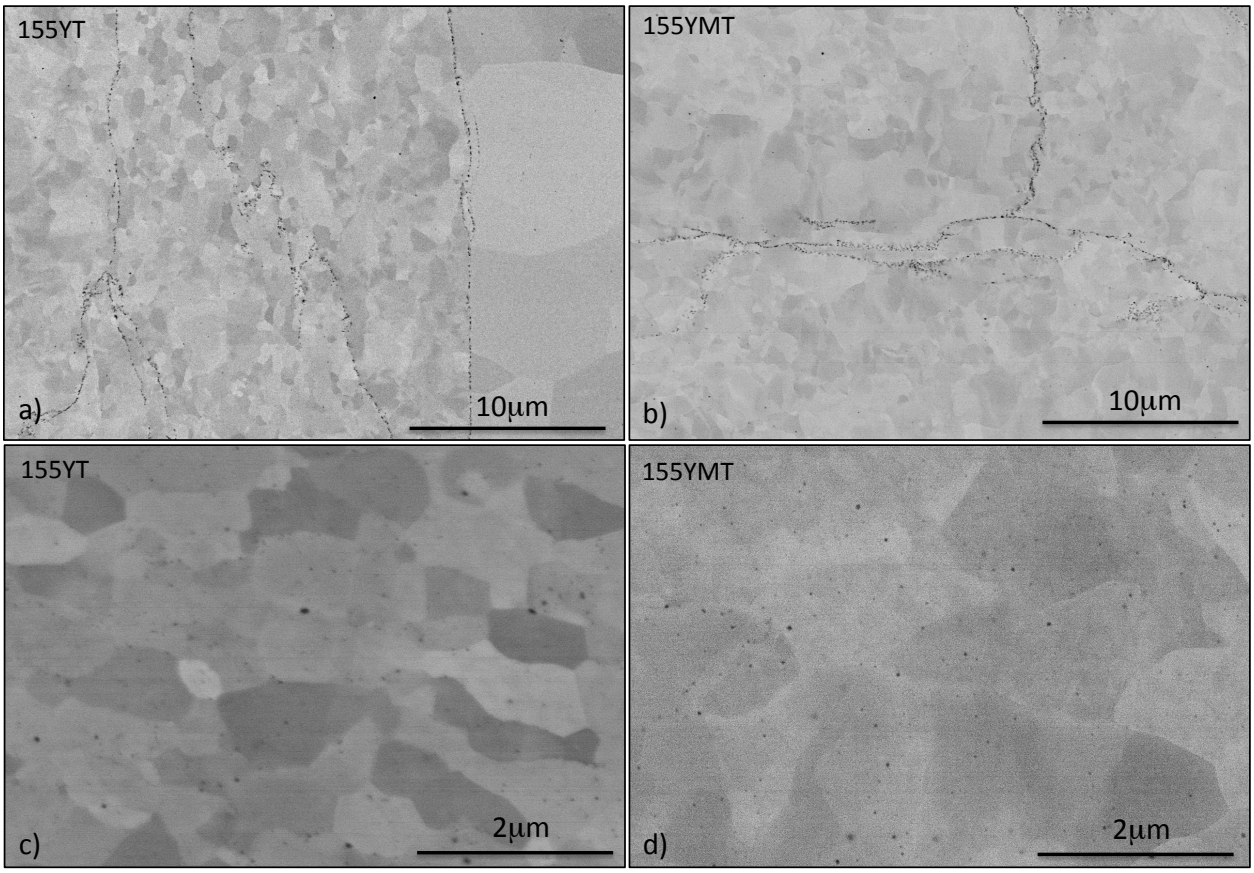


Fig. 1: SEM micrographs after extrusion, a) and c) alloy 155YT and b) and d) alloy 155YMT, showing a very small grain size with occasionally larger grains and the presence of a network of alumina stringers

The ultimate tensile strength (UTS) and plastic deformation at rupture for the two alloys are plotted as a function of the testing temperature in Figure 2. The two alloys exhibited similar behavior, with UTS in the 1000-1300MPa range up to 400ºC, and then a quasi linear decrease of the alloy strength down to ~310MPa at 800ºC. The data advertised by Plansee in their datasheet for alloy PM2000 as well as tensile data generated at ORNL from a 60mm dia. PM2000 rod were added for comparison in Figure 2. Alloy PM2000 was mainly considered for application at temperature over 900ºC where creep resistance is required. To improve the alloy creep strength, alloy PM2000 was exposed to 1h at 1380ºC to recrystallize the materials and form very large grains, up to 100mm in size. This treatment also significantly affects the

alloy tensile properties; the UTS of the coarse grain (CG) PM2000 does not exceed ~720MPa at room temperature and decreases nearly linearly with the temperature down to 110MPa at 800ºC. The small grain structure (SM) PM2000 was significantly stronger at low temperature and the UTS reached 1200MPa at room temperature, a value very close to the UTS of the 155YT and 155YMT alloys. However, the UTS decreased quickly above 400ºC and both the small and coarse grain PM2000 exhibited a similar UTS value at 800°C, ~110MPa. In comparison, the UTS was still ~350MPa for the 155YT and 155YMT alloys at 800°C. The weaker SG and CG PM2000 alloys are, however, more ductile at high temperature, reaching ~35% plastic deformation compared with ~12% for the 155Y(M)T alloys. The PM2000 alloy tested at ORNL showed tensile properties lying between the SG and CG PM2000 alloys. This alloy exhibits a small grain structure, ~1μm in diameter, but was meant to be recrystallized with a 1h 1380ºC treatment. The alloy was therefore not optimized for a small grain PM2000. Note however that the ORNL alloy showed a very high level of plastic deformation at rupture, over 100% at 800ºC. All the PM2000 alloys exhibited similar UTS values at 800ºC.

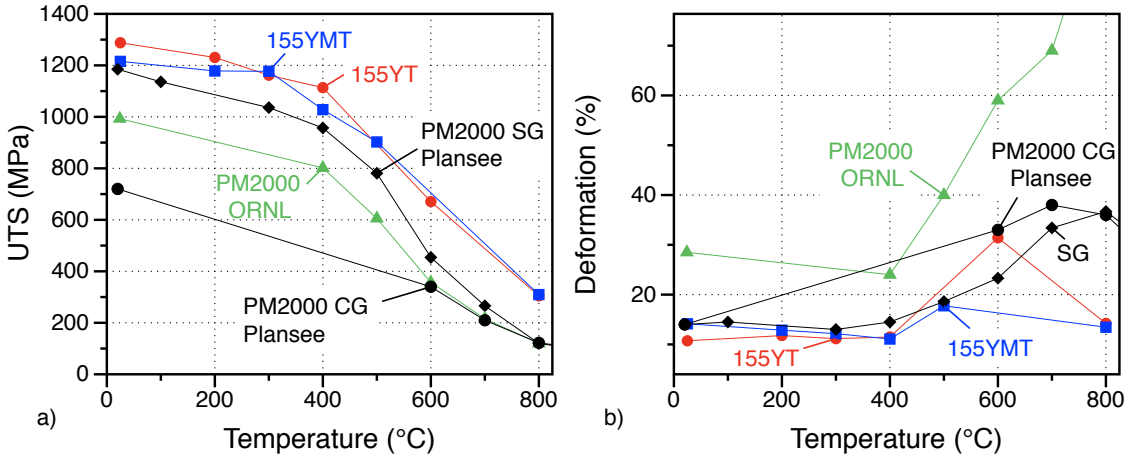


Fig. 2: Tensile properties of alloys 155YT, 155YMT and PM2000 from room to 800ºC, a) Ultimate tensile strength, b) Plastic deformation at rupture. Plansee data for alloy PM2000 in the small grain (SG) and coarse grain (CG) state are also plotted for comparison.

### 3.2 Annealed materials

The microstructure of the two alloys after exposure for 1000h at 800ºC and 1000ºC was characterized by SEM. At 800ºC, the microstructure was quite similar to the post extrusion microstructure. However, comparison between Figure 1 and Figure 3 shows that exposure at 1000ºC for 1000h resulted in a significant coarsening of the precipitates present in the stringers or networks of coarse precipitates. This is not surprising if these larger particles are mainly alumina. Many of the nano-precipitates also seem to have disappeared, see Figure 3c and 3d.

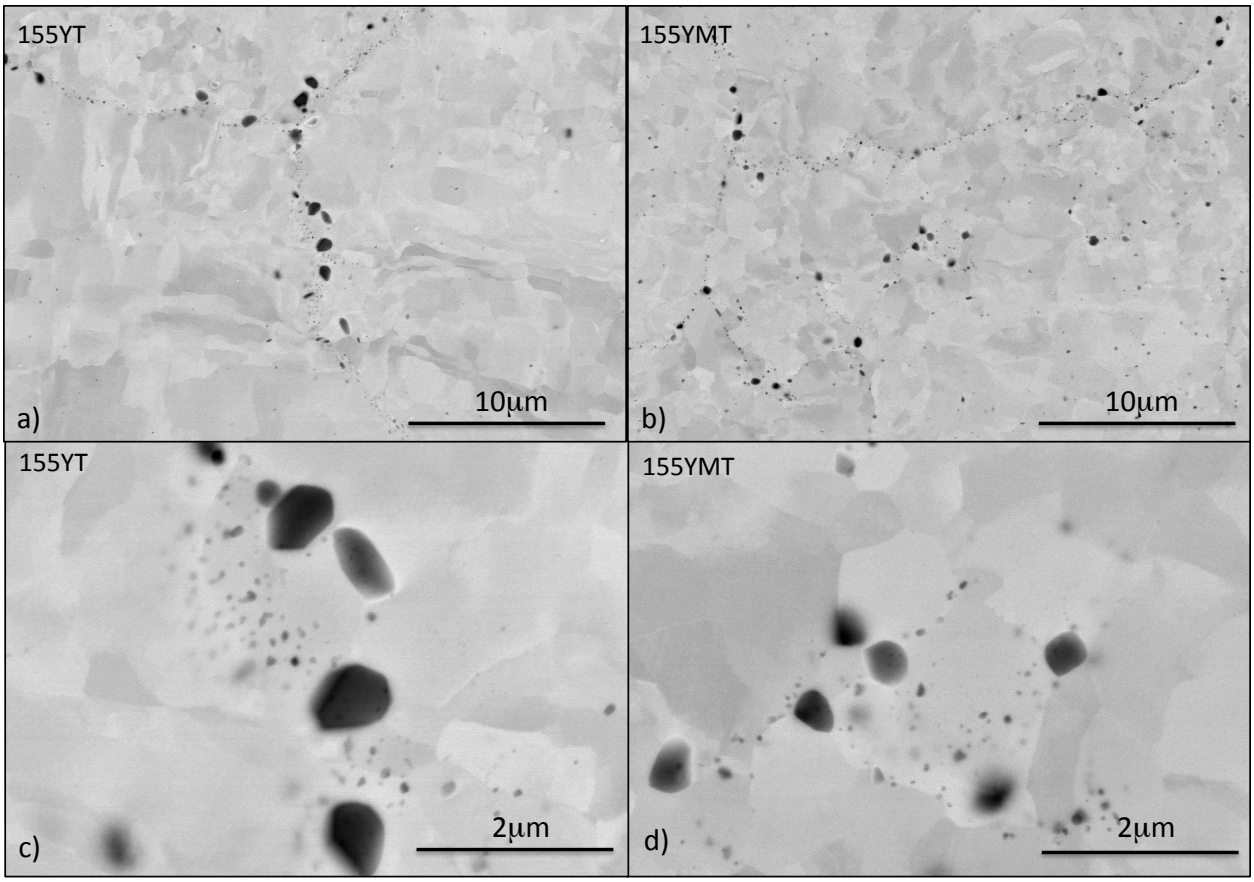


Fig. 3: SEM micrographs after exposure for 1000h at 1000ºC, a) and c) alloy 155YT, b) and d) alloy 155YMT, showing the coarsening of large precipitates and likely disappearance of smaller ones.

When annealed at 1200ºC for 100h, a partial recrystallization was observed with most of the grains several hundreds of micrometers in size, Figure 4, in addition to the precipitate coarsening observed at lower temperature. Some large voids can also be observed in Figure 4.

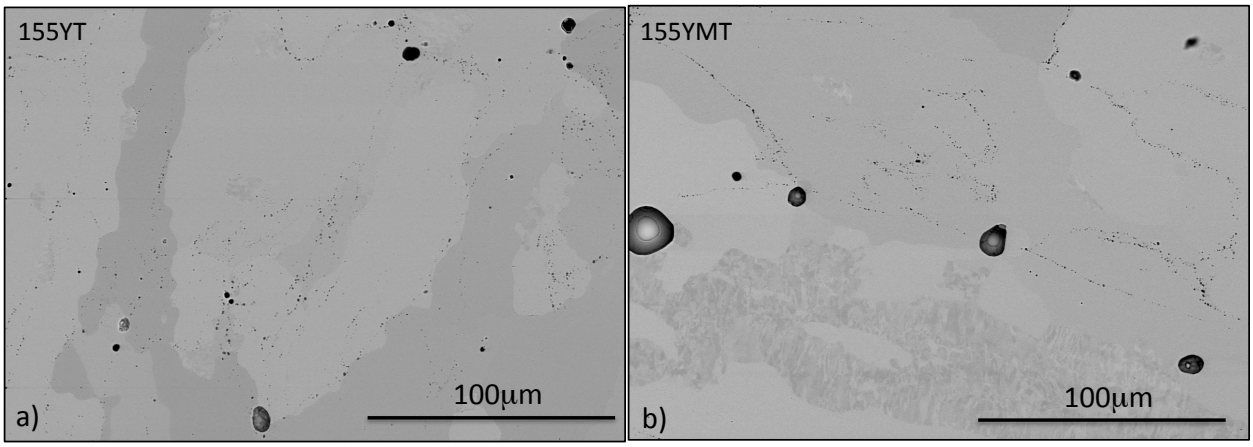


Fig. 4: SEM micrographs after exposure for 100h at 1200ºC, a) alloy 155YT and b) alloy 155YMT, showing a partial recrystallization of the alloys and the formation of large voids.

The two alloys were also heat treated at 1380ºC for 1h in an attempt to completely recrystallize the materials. The resulting microstructures shown in Figure 5 are very similar to the microstructure after

exposure for 100h at 1200ºC, with many large grains, islands of smaller grains, coarse precipitates and voids.

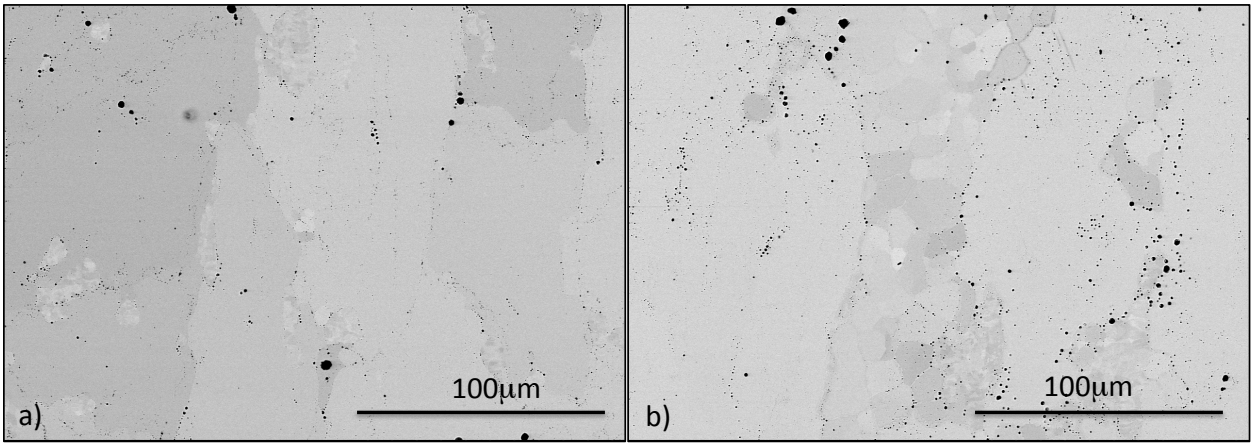


Fig. 5: SEM micrographs after exposure for 1h at 1380ºC, a) alloy 155YT and b) alloy 155YMT, showing partial recrystallization of the alloys

Vickers hardness values for alloys 155YT, 155YMT and ORNL PM2000 are compared in Figure 6 in the as extruded state and after annealing at 800ºC and 1000ºC. For all the alloys, a slight decrease in hardness was observed after 1000h at 800ºC, with a maximum drop of 20Hv for alloy 155YMT. The drop was significantly higher at 1000ºC for both the 155YT and 155YMT alloys, with hardness values down from ~375Hv to respectively ~320Hv and 300Hv after 100h and 1000h at 1000ºC. Alloy PM2000 was much more stable at 1000ºC, with only a small decrease of hardness from 350 to 330Hv after 1000h of exposure.

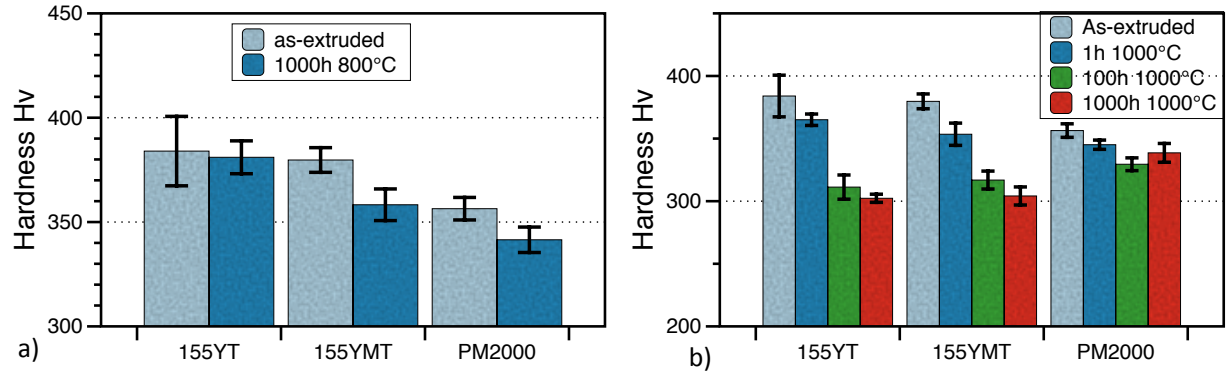


Fig. 6: Comparison of the hardness measurements for alloys 155YT, 155YMT and PM2000 after extrusion and, a) annealing at 800ºC for 1000h, b) annealing for 1h, 100h and 1000h at 1000ºC.

The tensile properties were also measured after the 1000h anneal, and Figure 7 shows the room temperature and 600ºC yield strength (YS) as a function of annealing temperature. As was observed for the hardness values, increasing the annealing temperature resulted in a decrease of the mechanical strength for the 155YT and 155YMT alloys but had little effect on alloy PM2000. Similar yield strength values were measured for the three alloys after exposure for 1000h at 1000ºC, ~800MPa at room

temperature and ~330MPa at 600ºC. All these results indicate that the microstructure responsible for the high strength of the two 155YT and 155YMT alloys after extrusion is not stable at high temperature, and 0.9 wt% Mo does not seem to affect the alloy tensile properties.

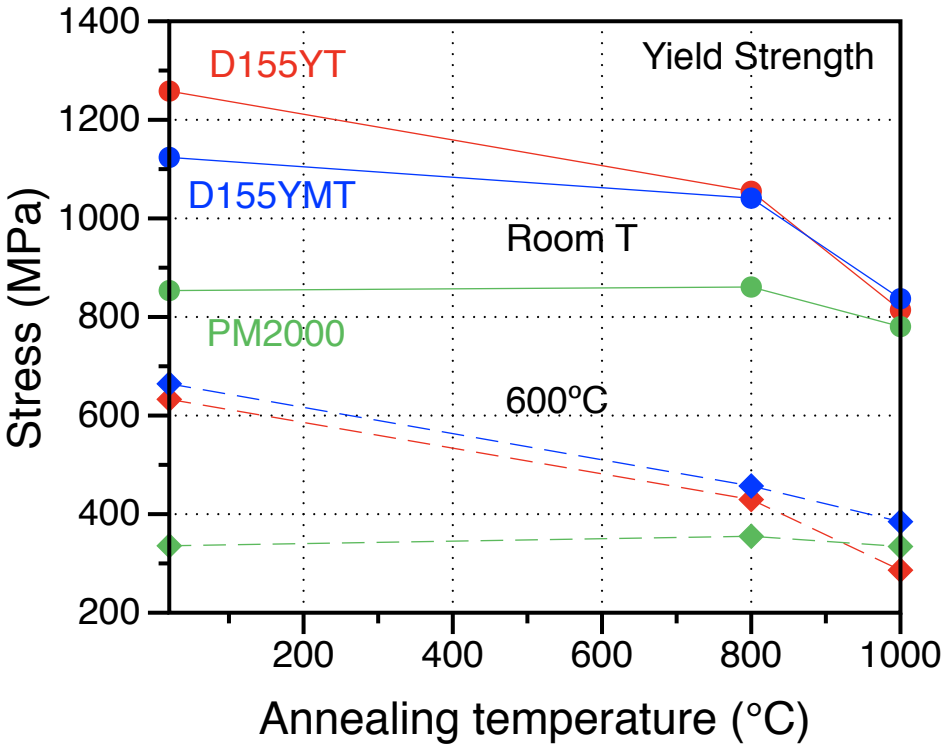


Fig. 7: Evolution of the yield strength with annealing temperature for alloys 155YT, 155YMT and PM2000, after exposure for 1000h.

### 3.3 High temperature oxidation behavior

The mass gains during isothermal exposure for 4h at 1200ºC are displayed in Figure 8 for the 155YT, 155YMT and two ODS 12Cr-5Al+$Y_2O_3$ alloys, one containing Hf (125YH) and the other one Zr (125YZ). The mass gains in steam for alloy APMT are also shown for comparison. In air, Figure 8a, all the mass gain curves looked similar except during the 1h transient period with higher mass gains for alloys 155YT and 155YMT. The curves obtained in steam are noisier but very similar to the curves generated in air. Table 2 lists the parabolic rate constant for each of the alloys. The APMT mass gain data are consistent with the ODS data.

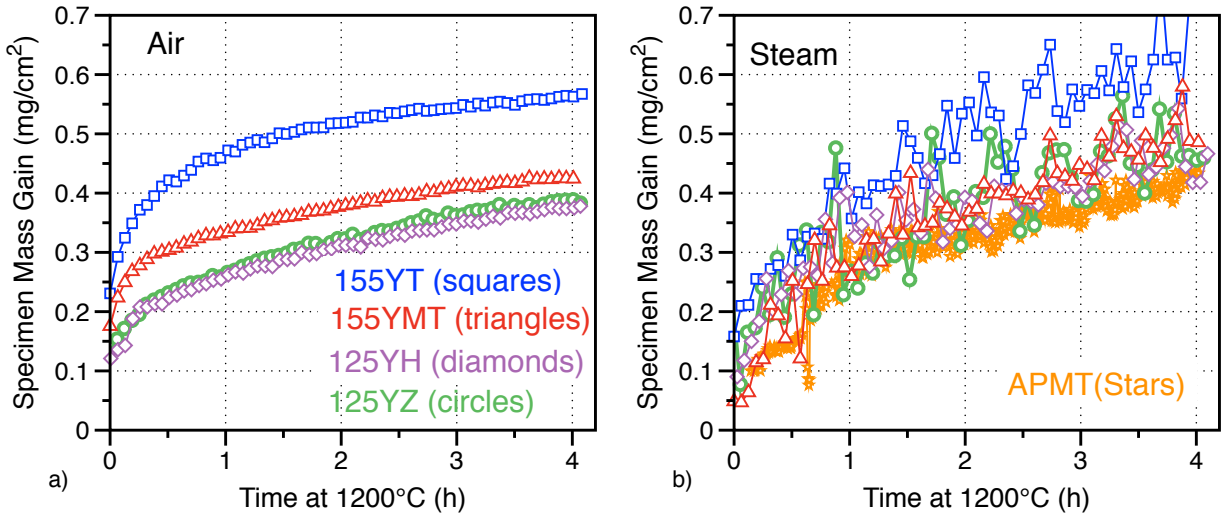


Fig.8: Specimen mass gain curves at 1200ºC for alloys 155YT, 155YMT, 125YH, 125YZ and APMT, a) air, b) steam

Table 2. Rate constants measured for alloys at 1200°C in steam and air

| Alloy | $k_p$ in air $g^2/cm^4s$ | $k_p$ in steam $g^2/cm^4s$ |
|---|---|---|
| 155YT | $4 \times 10^{-12}$ | $21 \times 10^{-12}$ |
| 155YMT | $3 \times 10^{-12}$ | $15 \times 10^{-12}$ |
| 125YH | $5 \times 10^{-12}$ | $9 \times 10^{-12}$ |
| 125YZ | $5 \times 10^{-12}$ | $10 \times 10^{-12}$ |
| APMT | n.a. | $5 \times 10^{-12}$ |

The mass gain data at 1200ºC were the first screening test for steam oxidation resistance, but do not convey the maximum capability of these ODS alloys. A ramp test was therefore conducted with the temperature being increased at a rate of 5ºC/min, and the resulting mass gains curves for the same alloys are shown in Figure 9. The onset of breakaway oxidation, with the formation of Fe-rich oxides, occurred for alloys 155YT and 155YMT at T~1380ºC. In general, ODS alloys do not appear to perform as well as wrought FeCrAl alloys of similar composition. The 125YZ specimen failed at a lower temperature, ~1325ºC, which was consistent with the lower Cr content in this alloy. However, the alloy 125YH specimen showed better behavior, failing at ~1470ºC, almost as high as the APMT specimen, which failed at ~ 1500ºC. Future work will further explore these results and attempt to determine how to push the maximum temperature closer to 1500°C for ODS alloys with lower Cr contents.

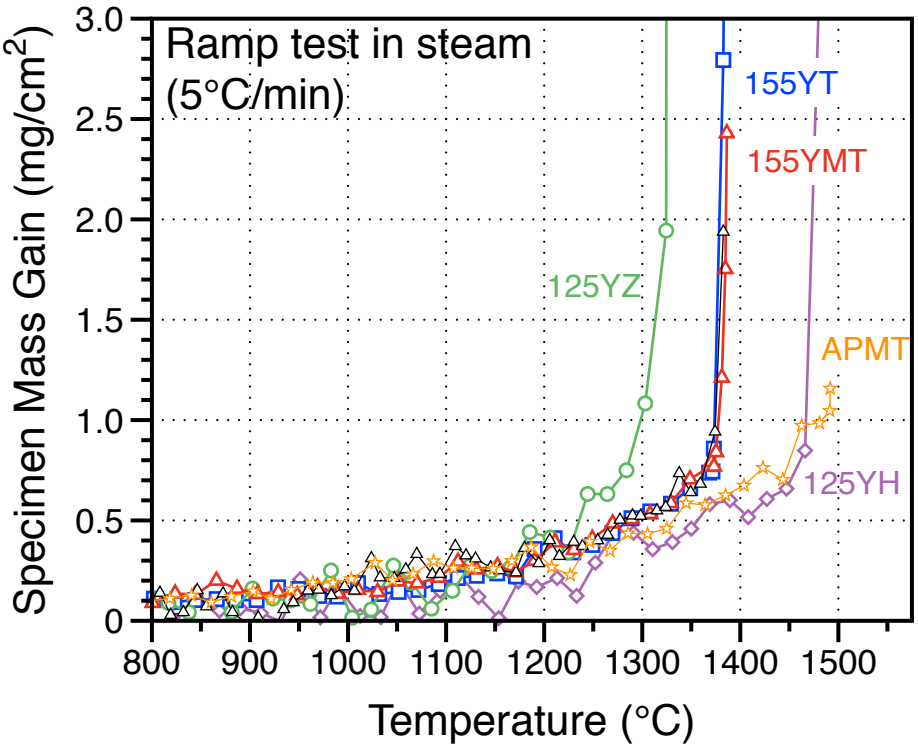


Fig.9: Ramp tests in steam for alloys 155YT, 15YMT, 125YZ, 125YH and APMT showing the alloy maximum temperature of use.

### 3.4 Creep behavior

Datasheets from Plansee and Sandvik indicate that at 800ºC, the SG PM2000 and APMT alloys should have a lifetime of ~1000h with applied stresses of respectively 50 and 25MPa. Because of the higher yield strength at 800ºC for all the alloys developed at ORNL, creep testing was conducted at 800ºC with applied stresses ranging from 65MPa to 100MPa, Figure 10. Alloy 155YMT ruptured after only ~35h both with applied stresses of 65 and 80MPa which indicates that the creep resistance of the alloy is likely similar to the creep resistance of SG PM2000 alloy. Alloy 155YT exhibited longer lifetimes at 800ºC and failed after 91h at 80MPa and has exceeded 375h at 65MPa. The creep performance of the 12Cr-5Al alloys was significantly better, with very low creep rates and a lifetime of 1200h for alloy 125YH at 100MPa. The 100MPa 800ºC creep test for alloy 125YZ has also exceeded 375h and is still on going.

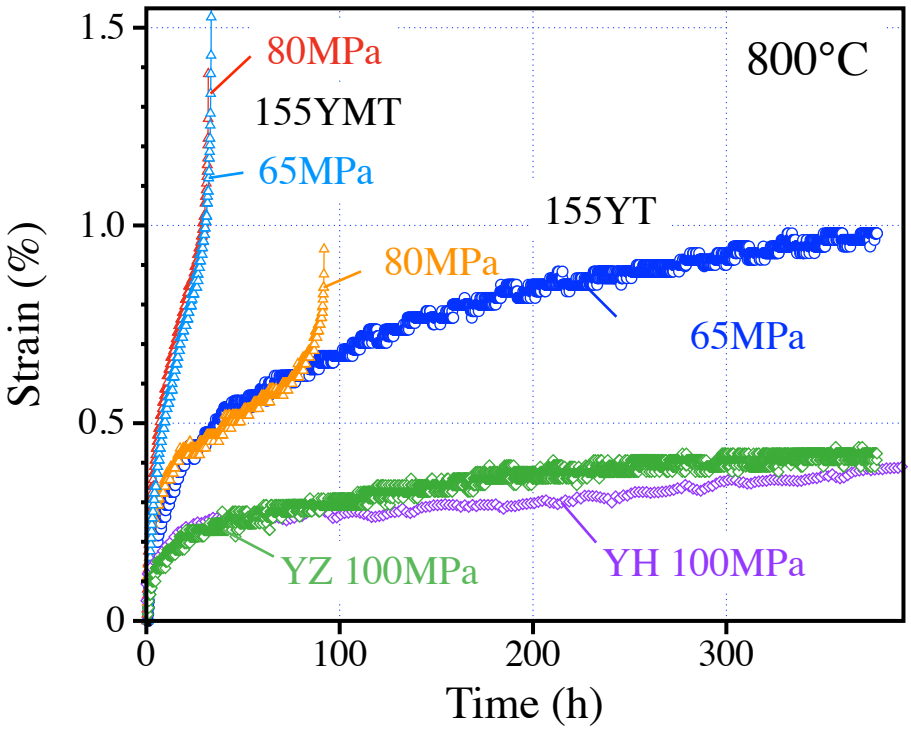


Fig.10: Creep curves at 800ºC for alloys 155YT and 155YMT, with applied stresses of 65 and 80MPa, and for alloys 125YZ and 125YH with an applied stress of 100MPa

## 4. Discussion and future work

155YT and 155YMT exhibit very good tensile properties up to 800ºC, which is likely due to the presence of nanometer scale Y-rich oxide precipitates and the very small alloy grain size. Dou et al. extruded an Fe-15.5Cr-2W-0.1Ti-4Al-0.35$Y_2O_3$ alloy at 1150ºC and 1050ºC,[12] and demonstrated that lowering the extrusion temperature resulted in smaller oxide particles, smaller grain size and higher hardness values. The 155YT and 155YMT alloys were extruded at 950ºC, and these results are consistent with Dou's data, with even smaller grains and higher hardness values, ~375Hv for our alloys and 356Hv and 327Hv for Fe–15.5Cr–2W–0.1Ti–4Al–0.35$Y_2O_3$ alloy extruded at respectively 1050 and 1150ºC. TEM characterization needs to be conducted to assess the nanoscale particle size of the 15Cr-5Al ODS alloys. It is worth noting that the yield strength of the two ODS alloys in the fuel cladding operating temperature range, 300-400ºC, is twice the yield strength of the best wrought FeCrAlY alloys developed at ORNL.

Despise the good tensile properties measured at 800ºC, the creep strength of the two 15Cr-5Al alloys at that temperature was similar or moderately better than the creep strength of SG PM2000. This is because the creep deformation at 800ºC is likely due to grain boundary sliding, which explains why the CG PM2000 exhibits a better creep resistance than the SG PM2000 above 800ºC, even if their tensile properties at 800ºC are similar. Recent work by Kimura et al. has shown that the addition of Zr and Hf can improve the creep properties of ODS Fe-16Cr-4Al alloy at 700ºC.[13] Their explanation was that the number density of oxides and carbides was greatly increased at grain boundaries with the addition of Hf or Zr, and these precipitates would prevent grain boundary sliding. We observed a similar creep improvement at 800ºC with the two 12Cr-5Al ODS alloys containing Zr or Hf. Adding Zr is therefore an interesting route to enhance the creep properties of the ODS cladding alloys, which could lead to a significant increase in the cladding burst resistance.

Although the 155YT alloy showed better creep resistance at 800ºC than the 155YMT alloy, it is not clear if the difference is due to a Mo effect. It was anticipated that Mo would improve creep strength by a solid solution strengthening mechanism. A smaller grain size was measured for alloy 155YT, which means that the precipitate size could also be smaller. Further work needs to be carried out to determine whether Mo has an effect on the final alloy microstructure or if a better control of the alloy fabrication process is required to systematically obtain the exact same microstructure.

The 15Cr-5Al wt% composition was selected because wrought FeCrAl alloys of similar composition were able to form a protective alumina scale in steam at 1200ºC. The ramp tests presented in Figure 9 show however that the maximum temperature of use for ODS FeCrAl alloys does not depend only on the Cr and Al contents. Alloy125YH was the only ODS alloy that reached 1480ºC. Further characterization of alloys 125YZ and 125YH will be conducted to help determine the reason for the higher maximum use temperature of the latter alloy.

The motivation for decreasing the level of Cr in the alloy down to 15Cr wt% was to limit the alloy embrittlement resulting from the formation of $\alpha$-Cr phase during irradiation and/or high temperature exposures. Steam testing of the 125YZ and 125YH alloys showed that the Cr content could be dropped down to ~12 wt% while still maintaining similar steam oxidation resistance. Further work will therefore be conducted to develop a new 12Cr-~5-6Al-Y-Zr ODS alloys with similar tensile and creep properties than the 125YZ alloy and a maximum ramp test temperature approaching 1500ºC.

Characterization of the two 155YT and 155YMT alloys after high temperature annealing has highlighted the alloy microstructure instability above ~1000ºC, and similar observations were reported for the 125YZr and 125YHf alloys.[14] However, as the application temperature is ~300°C for fuel cladding, the high temperature stability should not be a major concern.

## 5. Conclusion

Two Fe-15Cr-5Al-0.5Ti+$Y_2O_3$ ODS alloys, one of them containing ~1%wt Mo, were fabricated by powder ball milling followed by extrusion at 950ºC. The relatively low extrusion temperature resulted in a very fine grain structure for both alloys, leading to room temperature hardness values of 374Hv and 378Hv, and yield strengths of 1258MPa and 1124MPa for the 155YT and 155YMT alloys, respectively. Although the yield strengths at 800ºC of the two alloys were significantly higher than the yield strength of the small-grain PM2000, ~280MPa versus ~100MPa, the creep rupture life of the two 15Cr-5Al ODS alloys was only marginally superior to the creep resistance of the SG PM2000. The nanometer scale oxide precipitates present in the alloys were therefore not sufficient to prevent grain boundary sliding at 800ºC. A ramp test was used to estimate the maximum use temperature for the two alloys in steam, and both alloys failed at ~1380ºC, temperature ~100ºC lower than the temperature limit for similar wrought FeCrAlY alloys. Similar creep and ramp tests performed on 12Cr-5Al-$Y_2O_3$+Zr or Hf alloys developed for fusion applications have shown that a 12Cr-(5-6)Al-$Y_2O_3$-+Zr alloy could potentially exhibit high creep strength at 800ºC with maximum temperature of use in steam approaching 1500ºC.

## 6. Acknowledgments

The authors would like to thank M. Howell, A. Willoughby, T Jordan, T Geer, T. Lowe, C. Stevens, M. Stephens, J. Moser and D. Harper for their help with the experimental work. They want also to acknowledge Y. Yamamoto and J. Keiser for reviewing the manuscript. This research was sponsored by the U.S. Department of Energy, FCRD Advanced Fuels Campaign Program

## 7. References

[1] T. Cheng, J. R. Keiser, M. P. Brady, K. A. Terrani and B. A. Pint, "Oxidation of fuel cladding candidate materials in steam environments at high temperature and pressure," Journal of Nuclear Materials, 427, 396-400 (2012).

[2] K. A. Terrani, S. J. Zinkle, L. L. Snead, "Advanced oxidation-resistant iron-based alloys for LWR fuel cladding", Journal of Nuclear Materials, 448, 420-435 (2014).

[3] F.H. Stott, G.C. Wood, F.A. Golightly, "The isothermal oxidation behavior of Fe-Cr-Al and Fe-Cr-Al-Y at 1200ºC, Corrosion Science, 19, 869-887 (1979)

[4] B. A. Pint, K. A. Unocic and K. A. Terrani, "The Effect of Steam on the High Temperature Oxidation Behavior of Alumina-Forming Alloys," submitted to Materials at High Temperature.

[5] B. A. Pint, K. A. Terrani, J. R. Keiser, M. P. Brady, Y. Yamamoto and L. L. Snead, "Material Selection for Fuel Cladding Resistant to Severe Accident Scenarios," NACE Paper ED2013-3083, Houston, TX, presented at the 16th Environmental Degradation conference, Asheville, NC, August 2013.

[6] M. Mathon, Y. De Carlan, G. Geoffroy, X. Averty, A. Alamo, C. De Novion, "A SANS investigation of the irradiation-enhanced α–α' phases separation in 7–12 Cr martensitic steels," Journal of Nuclear Materials 312 (2003) 236.

[7] N.M. George, K.A. Terrani, J.J. Powers, "Neutronic analysis of candidate accident-tolerant iron alloy cladding concepts", ORNL report TM-2013/121 (2013).

[8] Y. Yamamoto, Y. Yang, K.G. Field, K. Terrani, B.A. Pint, L.L. Snead, "*Letter Report Documenting Progress of Second Generation ATF FeCrAl Alloy Fabrication*," FY14 FCRD milestone report, M3FT-14OR0202232, ORNL/LTR-2014/219 (2014).
[9] S. Ikeda, S. Ohashi and G. Ito, " Effect of Titanium and Molybdenum Addition on the Oxidation Resistance and Mechanical Properties of Fe-Cr-Al Alloys", Transaction of National Research Institute for Metals, 15, 29-35 (1973).
[10] C.Gaspard, E. Diderrich, V. Leroy, JJ Huet and L. Habraken "Fe- 13 Cr-Ti-Mo Ferritic Alloy as Material for a Fast Reactor", Journal of Nuclear Materials, 68, 104-110 (1979).
[11] J.J. Fischer, "Dispersion strengthened ferritic alloy for use in liquid-metal fast breeder reactors (LMFBRS)". 4,075,010 United States Patent, 21 February 1978. assigned to The International Nickel Company, New York, NY.
[12] P. Dou, A. Kimua, T. Okuda, M. Inoue, S. Ukai, S. Ohnuki, T. Fujisawa and F. Abe, "Effects of extrusion temperature on the nano-mesoscopic structure andmechanical properties of an Al-alloyed high-Cr ODS ferritic steel", Journal of Nuclear Materials, 417, 166-170 (2011).
[13] A. Kimura, R. Kasada, N. Iwata, H. Kishimoto, C.H. Zhang, J. Isselin, P. Dou, J.H. Lee, N. Muthukumar, T. Okuda, M Inoue, S. Ukai, S. Ohnuki, T. Fujisawa and T.F. Abe, "Development of Al added high-Cr ODS steels for fuel cladding of next generation nuclear systems", Journal of nuclear materials, 417, 176-179 (2011).
[14] B. A. Pint, K. A. Unocic, S. Dryepondt and D. T. Hoelzer, Development of ODS FeCrAl for fusion application, Fusion Reactor Materials Program, DOE/ER-0313/56–Volume 56, 31-38 (2014).